

Search for long-range force between a neutron and an atom with a trap of ultracold neutrons

A. P. Serebrov,* O. M. Zhrebtsov, S. V. Sbitnev, V. E. Varlamov, A. V. Vassiljev, and M. S. Lasakov
 Petersburg Nuclear Physics Institute, Russian Academy of Sciences, Gatchina, Leningrad District, 188300, Russia
 (Received 5 August 2010; revised manuscript received 3 August 2011; published 17 October 2011)

A method of using a gravitational ultracold neutron (UCN) spectrometer for the search for long-range forces between neutrons and atoms is proposed. The constraints on the strength of long-range forces within the range of 10^{-10} – 10^{-4} cm can be obtained from experiments on measurements of the total cross section of the interaction of UCN with atoms of noble gases (He, Ne, Ar, Kr) and data on the coherent neutron-scattering length of the nucleus. The first result of such an analysis is presented. Further prospects for the UCN method are discussed.

DOI: [10.1103/PhysRevC.84.044001](https://doi.org/10.1103/PhysRevC.84.044001)

PACS number(s): 29.90.+r, 28.20.-v, 04.80.-y, 14.80.-j

I. INTRODUCTION

The search for deviations of gravitational interaction from the $1/r^2$ law (inverse-square law) in the range of small distances is extremely important to verify both theories assuming the existence of additional dimensions [1,2] and supersymmetric theories in which the existence of new very light particles is assumed. The exchange of these particles leads to additional interactions between nucleons [3–5]. A review of theoretical and experimental works on the search for deviations from the inverse-square law is presented in Refs. [6,7]. In this paper we will discuss forces that can appear at distances of 10^{-10} – 10^{-4} cm. From the point of view of the search for deviations of gravitational interaction from the inverse-square law these forces should be defined as short-range forces. But in nuclear interactions there is a characteristic scale of distances of the order of 10^{-13} cm, therefore for nuclear physics the interaction at distances of 10^{-10} – 10^{-4} cm is carried on by long-range forces. We have defined these forces as long-range forces because it is a question of the interaction of a neutron with a nucleus.

There are different methods of searching for long-range forces in the interaction of elementary particles [6–8]. Within the range of 10^{-11} – 10^{-9} cm investigations are carried out by means of neutrons at an energy of the order of electron volts [9,10]. For distances 10^{-4} – 10^{-2} cm the laboratory experiments on the gravitational interactions of bodies are performed [11–20]. Within the range of 10^{-10} – 10^{-4} cm there are rather effective methods using thermal and cold neutrons [9,21]. The present paper will discuss the possibility of using ultracold neutrons (UCNs) for the range 10^{-10} – 10^{-4} cm.

The scattering amplitude of a neutron by atoms can be expressed in the following way:

$$f(q) = f_{\text{nucl}} + f_{n-e}(q) + f_{\text{long-range}}(q), \quad (1)$$

where f_{nucl} is a nuclear scattering amplitude, which is usually expressed in terms of scattering length b , $f_{\text{nucl}} = -b$, and $f_{n-e}(q)$ is the amplitude of neutron-electron scattering, which arises due to neutron scattering by charges distributed inside the nucleus and the electron shell of atoms. Further we will not consider contribution from $n-e$ interactions because this effect

occurs mainly for fast neutrons [22]. The last term in Eq. (1) relates to a hypothetical long-range interaction (compared to the nuclear one) of a neutron with a nucleus; $f_{\text{long-range}}(q)$ is a spin-independent amplitude of interaction, which is likely to arise as a result of exchange by a scalar or vector boson. In the case of the scalar type of interaction the potential of interaction is written as an attractive potential; for a vector boson exchange the potential of interaction is written as a repulsive one.

$$\varphi(r) = \frac{\pm g_{\pm}^2 M \hbar c e^{-r/\lambda}}{4\pi r}, \quad (2)$$

where M is the mass of the interacting particle expressed in units of nucleon mass m_n , λ is the effective radius of interaction, and g_{\pm}^2 is a dimensionless coupling constant. It should be noted that in the general case $M = m_1 m_2 / m_n^2$, where m_1 and m_2 are masses of interacting particles. In our consideration we have assumed that the protons and neutrons in the atom couple equally to the free neutron via the long-range force and that the electrons do not couple to the free neutron. In formula (2) the upper sign corresponds to a vector type of interaction, whereas the lower sign corresponds to a scalar type of interaction.

In a similar way, the amplitude within the Born approximation can be presented in the form

$$\begin{aligned} f_{\text{long-range}}(q) &= -\frac{m}{2\pi\hbar^2} \int \varphi(r) e^{-i\vec{q}\vec{r}} dV \\ &= \frac{\mp 2m g_{\pm}^2 M \hbar c}{\hbar^2} \frac{\lambda^2}{4\pi (\lambda q)^2 + 1}, \end{aligned} \quad (3)$$

where m is a reduced mass $m = \frac{m_n m_A}{m_n + m_A}$, the mass of an atom of gas $m_A = m_n M$, $q = |\vec{k}' - \vec{k}|$ is the momentum transferred to a neutron, and \vec{k} and \vec{k}' are wave vectors of the neutron within the center of mass before and after collision. The momentum q is bound with the neutron recoil energy ε by a simple ratio: $q = \frac{\sqrt{2\varepsilon m_n}}{\hbar}$.

An experimental search for additional terms in the scattering amplitude can be based on the fact that a long-range interaction contributes to the scattering amplitude either at small transferred momentum q or at small scattering angles.

* serebrov@pnpi.spb.ru

The scattering amplitude at $\theta = 0$ or $q = 0$ can be measured at high accuracy in neutron-optical experiments with an interferometer [21]. This result should be compared with $f_{\text{nucl}} = -b$ to find the presence of additional terms in Eq. (1). For example, comparing measurements by interferometers and experiments with the Bragg diffractometer allows us to obtain restrictions [9] that are strong enough.

Recently, the method of studying quantum states of a neutron in Earth's gravitational field near the matter surface [23] has been actively discussed. However, there is lack of real statistics in this research; therefore we are going to propose a more statistical method in this paper.

A direct method of research would be the method of small-angle scattering, as the existence of long-range forces results in scattering occurring at small angles. In this method there are obvious problems caused by the existence of small-angle scattering resulting from scattering on the texture of the matter and multiple scattering. In addition, the initial divergence of a beam does not permit us to distinguish scattering at very small angles from the beam divergence.

This paper suggests reconsidering the approach to the method of small-angle scattering and using the registration of small-recoil energy instead of small angles of scattering. This approach suggests using a gas of UCNs as a target that collides with the flux of atoms in the same trap. The criterion of a signal of the scattering induced by long-range forces is a transfer of the ultimately small recoil energy of $\sim 10^{-7}$ eV, registered with a trap of ultracold neutrons.

For thermal neutrons the recoil energy to a neutron of $\sim 10^{-7}$ eV corresponds to a scattering angle of $\sim 2 \times 10^{-3}$ rad, which is within the divergence of an incident neutron beam. For cold neutrons this scattering angle is twice as high, but it does not yet exceed the divergence of a neutron beam.

The method of an ultracold neutron trap filled with the investigated gas (He, Ne, Ar, or Kr) allows a recoil energy of about 10^{-7} eV to be registered. On the other hand, the total cross section of a UCN with a gas will not involve areas with recoil energy smaller than 10^{-7} eV. Thus, it is possible to compare the scattering amplitude from interferometer measurements $f(0)$ with the amplitude obtained by the UCN method.

II. EXPERIMENTAL SETUP

One of the possible schemes of an experiment is shown in Fig. 1. It enables us to use the available equipment of Petersburg Nuclear Physics Institute (PNPI) in Institut Laue-Langevin (ILL). UCNs fill the trap (3) at an opened valve (2) and closed valves (5). The absorber (4) is placed in the bottom position at a distance h from the trap bottom. When equilibrium density in the trap is achieved, the valve (2) is closed. There are two foils installed at the trap entrance and the trap exit. The critical energy of the foils is $E_{\text{UCN}}^{\text{foil}} = m_n g h$.

Foils can be installed in the UCN guide or removed from the UCN guide. They will be used sometimes for forming the UCN spectrum at the trap entrance and for analysis of the UCN spectrum at the trap exit. Normally, UCNs fill the trap when the entrance foil is removed. The UCNs are stored in the trap for a predetermined time t_{hold} to form the spectrum with maximal UCN energy equal to $m_n g h$. Then the absorber

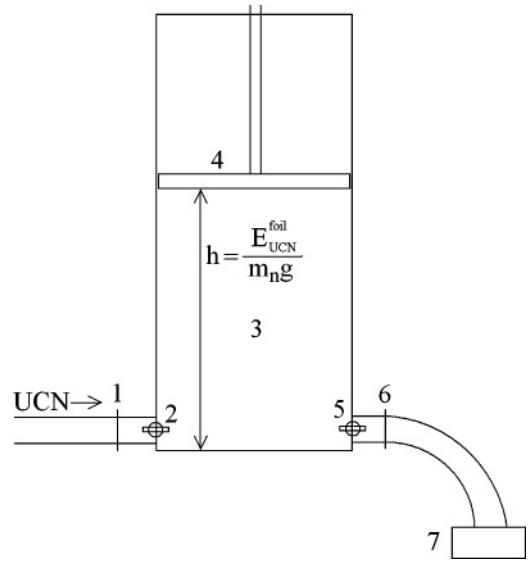


FIG. 1. The experiment setup: 1, entrance foil with critical energy $E_{\text{UCN}}^{\text{foil}} = m_n g h$; 2, the entrance valve; 3, UCN trap with the critical energy $E_{\text{UCN}}^{\text{trap}}$; 4, the absorber for formation of UCN spectrum; 5, the exit valve; 6, exit foil with critical energy $E_{\text{UCN}}^{\text{foil}} = m_n g h$; 7, the UCN detector.

(4) is pulled up to the upper position near the top of the trap.

Ultracold neutrons interact with trap walls and with the investigated gas, which fills the trap. The trap and the investigated gas are maintained at room temperature. The temperature of the UCN gas is 10^{-3} K. In coherent reflection from matter the energy of the UCN is conserved. Inelastic scattering occurs when a neutron is scattered by atoms of gas and when UCNs penetrate into the substance reflecting from the wall. In both cases there is energy transfer on the order of kT . Energy transfer of the order of 10^{-7} eV is of low probability for the above-mentioned processes. Nevertheless, in reflecting from the substance there is a quasielastic scattering that was revealed experimentally [24]. Due to the long-range interaction with atoms of gas a quasielastic scattering at a recoil energy of the order of 10^{-7} eV would be also possible. Processes of energy transfer of the order of kT and $\sim 10^{-7}$ eV are easily distinguished in the present installation, as UCNs that have obtained energy $\sim kT$ leave an experimental trap. Such neutrons are not detected. Neutrons that have obtained a small recoil energy can still be stored in the trap if their energy near the bottom is less than critical energy of the trap. The critical energy of the foil is equal to $m_n g h$. Therefore neutrons that have obtained a small recoil energy can overcome the potential barrier of the foil (6) and finally can be registered by a detector (7). For the registration of these neutrons the valve (5) is opened just after lifting the absorber. The closed valve (5) is used for measuring the background at the detector (7). To distinguish between the processes of quasielastic scattering on the surface of the trap and scattering with the investigated gas, measurements are to be made both with the investigated gas and without it. The above-described scheme of measurement permits us to determine an extremely low

energy transfer. Such a scheme was used in our measurements of lower-energy up scattering of UCNs from the trap walls [24].

For measuring the total cross section of UCN interaction with a gas the detector (7) is applied to measure the number of UCNs in the trap after different holding times with a closed valve (5). In this case the foil (6) is removed from the guide. Measuring UCN storage time at different gas pressures, we can determine the total cross section of UCN interaction with atoms. The measurement of UCN storage time in the trap τ_{stor} is a conventional procedure. It consists of measurements of the number of UCNs in the trap $N(t_1)$ at the moment t_1 after closing the entrance valve (2) and the number of UCNs in the trap $N(t_2)$ at the moment t_2 . The storage time τ_{stor} is determined according to the formula $\tau_{\text{stor}} = \ln[N(t_1)/N(t_2)]/(t_2 - t_1)$. As UCNs are sensitive to a small energy transfer, this cross section will include the interaction induced by long-range forces. We can compare the obtained results with the nuclear scattering cross section.

Summing up, one can conclude that two experimental methods have been discussed: the method of total cross-section measurements where the exit foil (6) is not used and the method of above-barrier neutron measurements using the exit foil (6). The potential sensitivity of both methods will be discussed below.

III. NUMERICAL CALCULATIONS AND ESTIMATIONS

Let us calculate the differential cross section depending on the recoil energy transferred to the ultracold neutron. To simplify the problem we will assume an UCN before collision to be at rest. The atoms of gas are scattered on UCNs. Neutrons obtain the recoil energy. We will consider the amplitude of an additional long-range interaction of a neutron with an atom consisting of M nucleons.

The differential cross section of scattering of a neutron with an atom should take into account the amplitude of nuclear

scattering and that of scattering (3) due to an additional contribution from potential (2):

$$\begin{aligned} d\sigma &= |f_{\text{nucl}} + f_{\text{long-range}}|^2 d\Omega \\ &= \left(b_{\text{free-nucl}}^2 \pm \frac{g_{\pm}^2 M b_{\text{free-nucl}} m c^2}{\pi \hbar c} \frac{\lambda^2}{(\lambda q)^2 + 1} \right. \\ &\quad \left. + f_{\text{long-range}}^2 \right) d\Omega, \end{aligned} \quad (4)$$

where the element of solid angle $d\Omega$ is bound with the energy of an incident atom E_A according to the following formula:

$$d\Omega = \frac{\pi (M + 1)^2 d\varepsilon}{M E_A}. \quad (5)$$

For the differential cross section the following expression has been derived:

$$\begin{aligned} d\sigma &= \pi \left[\frac{(M + 1)^2}{M} b_{\text{free-nucl}}^2 \pm \frac{g_{\pm}^2 M (M + 1) b_{\text{free-nucl}} m_n c^2}{\pi \hbar c} \right. \\ &\quad \times \frac{\lambda^2}{2m_n \varepsilon \lambda^2 / \hbar^2 + 1} + \frac{g_{\pm}^4 M^3 \lambda^4}{4\pi^2} \left(\frac{m_n c}{\hbar} \right)^2 / \\ &\quad \left. \times (2m_n \varepsilon \lambda^2 / \hbar^2 + 1)^2 \right] \frac{d\varepsilon}{E_A}. \end{aligned} \quad (6)$$

Figures 2(a) and 2(b) show the dependence of the differential cross section of scattering on the recoil energy for two different cases, $\lambda = 10^{-8}$ cm and $\lambda = 10^{-6}$ cm, for a repulsive and an attractive potential, respectively. The given calculations have been made in Fig. 2 for the fixed energy of an incident atom of helium equal to 2.5×10^{-2} eV. For $\lambda = 10^{-8}$ the differential scattering cross section spans the full range of energies from 0 to $\varepsilon_{\text{max}} = E_A 4M / (1 + M)^2$. At $\lambda = 10^{-6}$ cm, the differential cross section changes rapidly at recoil energies of the order of 10^{-7} eV. At $\lambda = 10^{-4}$ cm recoil energies at which the long-range forces will give a sensible contribution to the cross section are too small.

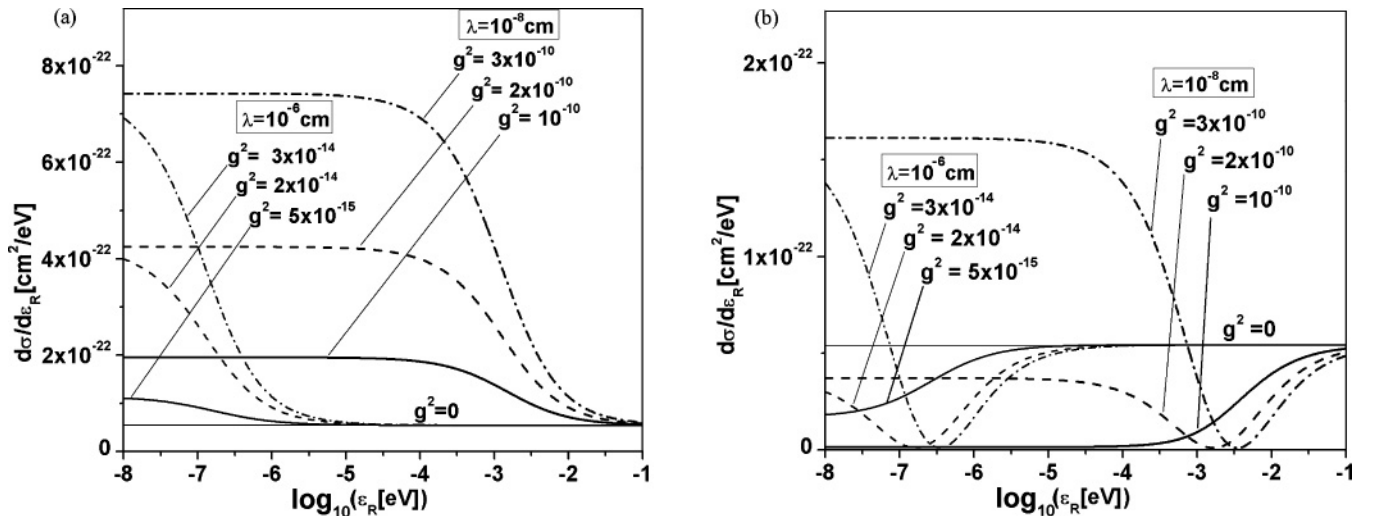


FIG. 2. Dependence of the differential cross section on recoil energy ε_R transferred to a neutron for various values of parameter 1. (a) The case of a repulsive potential and (b) the case of an attractive potential.

Now we will integrate expression (6) over a recoil energy from ε_1 up to ε_2 .

$$\sigma(\varepsilon_2, \varepsilon_1, E_A) = \pi \left[\frac{(M+1)^2}{M} b_{\text{free-nucl}}^2 (\varepsilon_2 - \varepsilon_1) \pm g_{\pm}^2 M \frac{\hbar c b_{\text{free-nucl}} (M+1)}{2\pi} \ln \left(\frac{2m_n \lambda^2 \varepsilon_2 / \hbar^2 + 1}{2m_n \lambda^2 \varepsilon_1 / \hbar^2 + 1} \right) + (g_{\pm}^2 M)^2 \left(\frac{m_n c}{2\pi \hbar} \right)^2 \frac{M \lambda^4 (\varepsilon_2 - \varepsilon_1)}{(2m_n \lambda^2 \varepsilon_2 / \hbar^2 + 1)(2m_n \lambda^2 \varepsilon_1 / \hbar^2 + 1)} \right] \frac{1}{E_A}. \quad (7)$$

The integral UCN scattering cross section when UCNs escape from the trap with critical trap energy $E_{\text{UCN}}^{\text{trap}}$ is

$$\sigma^{\text{escape}}(E_{\text{UCN}}^{\text{trap}}, E_A) = \pi \left\{ 4b_{\text{free-nucl}}^2 \left[1 - \frac{E_{\text{UCN}}^{\text{trap}} (M+1)^2}{4E_A M} \right] \pm g_{\pm}^2 M \frac{\hbar c b_{\text{free-nucl}} (M+1)}{2\pi E_A} \ln \left[\frac{8m_n \lambda^2 E_A M / \hbar^2 (M+1)^2 + 1}{2m_n \lambda^2 E_{\text{UCN}}^{\text{trap}} / \hbar^2 + 1} \right] + (g_{\pm}^2 M)^2 \left[\frac{m_n c M}{\pi \hbar (M+1)} \right]^2 \frac{\lambda^4 \left[1 - E_{\text{UCN}}^{\text{trap}} (M+1)^2 / 4E_A M \right]}{[8m_n M \lambda^2 E_A / (M+1) \hbar^2 + 1] (2m_n \lambda^2 E_{\text{UCN}}^{\text{trap}} / \hbar^2 + 1)} \right\}. \quad (8)$$

The lower-energy UCN scattering cross section when UCNs are still stored in the trap is

$$\sigma^{\text{low}}(E_{\text{UCN}}^{\text{trap}}, E_A) = \pi \left[\frac{(M+1)^2}{M} b_{\text{free-nucl}}^2 \frac{E_{\text{UCN}}^{\text{trap}}}{E_A} \pm g_{\pm}^2 M \frac{\hbar c b_{\text{free-nucl}} (M+1)}{2\pi E_A} \ln (2m_n \lambda^2 E_{\text{UCN}}^{\text{trap}} / \hbar^2 + 1) + (g_{\pm}^2 M)^2 \left(\frac{m_n c}{2\pi \hbar} \right)^2 \frac{M \lambda^4 E_{\text{UCN}}^{\text{trap}} / E_A}{(2m_n \lambda^2 E_{\text{UCN}}^{\text{trap}} / \hbar^2 + 1)} \right]. \quad (9)$$

The total scattering cross section of UCN with an atom is

$$\sigma_{\text{scatt}}^{\text{total}}(E_A) = \pi \left\{ 4b_{\text{free-nucl}}^2 \pm g_{\pm}^2 M \frac{\hbar c b_{\text{free-nucl}} (M+1)}{2\pi E_A} \ln [8m_n \lambda^2 E_A M / \hbar^2 (M+1)^2 + 1] + (g_{\pm}^2 M)^2 \left[\frac{m_n c M}{\pi \hbar (M+1)} \right]^2 \frac{\lambda^4}{8m_n M \lambda^2 E_A / (M+1) \hbar^2 + 1} \right\}. \quad (10)$$

It should be mentioned that for the sake of simplification we have assumed initial UCN energy to be equal to zero. Such a simplification does not matter, but it makes the calculation much easier. Formulas (7)–(10) are written for the fixed kinetic energy of an atom. For further calculations we should integrate over the flux of incident atoms. As has been noted above, the installation setup enables us to measure the total cross sections of the interaction of UCNs with a gas using the detector without the exit foil (6) and the differential cross sections of a very small energy transfer using the detector with the exit foil (6). In the following section the first experimental observables are considered in detail.

IV. MEASURING THE TOTAL INTERACTION CROSS SECTION OF A NEUTRON AND ATOMS OF A GAS

The probability of UCN storage in a trap is the sum of probability of UCN losses:

$$\tau_{\text{stor}}^{-1\text{total}} = \tau_n^{-1} + \tau_{\text{stor}}^{-1\text{gas}} + \tau_{\text{stor}}^{-1\text{walls}}, \quad (11)$$

where τ_n^{-1} is the neutron decay probability, $\tau_{\text{stor}}^{-1\text{gas}}$ is the probability of UCN losses due to interaction with gas atoms, and $\tau_{\text{stor}}^{-1\text{walls}}$ is the probability of UCN losses due to interaction with the trap walls.

The probability of UCN losses caused by neutron interaction with gas atoms can be measured as the difference of UCN

storage probability in a trap with gas density n_A and with zero gas density:

$$\tau_{\text{stor}}^{-1\text{gas}}(n_A) = \tau_{\text{stor}}^{-1\text{total}}(n_A) - \tau_{\text{stor}}^{-1\text{total}}(n_A = 0). \quad (12)$$

Now let us calculate the magnitude of the value of $\tau_{\text{stor}}^{-1\text{gas}}(n_A)$, taking into account an additional contribution made by the long-range interaction. The probability of UCN losses induced by collision with gas atoms can be written as follows:

$$\tau_{\text{stor}}^{-1\text{gas}}(n_A) = \int_{E_{\text{min}}}^{\infty} d\Phi(E_A) \int_{\varepsilon_{\text{min}}}^{E_A \frac{4M}{(M+1)^2}} d\sigma(\varepsilon) + n_A V_{2200} \sigma_{\text{capt}}^0 = n_A \bar{V}_A \sigma_A^{\text{total}}, \quad (13)$$

where $d\Phi(E_A)/dE_A$ is a flux of atoms incident on an ultracold neutron, $d\sigma/d\varepsilon(\varepsilon)$ is a differential cross section depending on the recoil energy, according to formula (6), σ_{capt}^0 is the capture cross section reduced to neutron velocity $V_{2200} = 2.2 \times 10^5 \text{ cm s}^{-1}$, and σ_A^{total} is the total cross section, which consists of the scattering cross section σ_{scat} and the capture cross section σ_{capt}^0 : $\sigma_A^{\text{total}} = \sigma_{\text{scat}} + \sigma_{\text{capt}}^0 V_{2200} / \bar{V}_A$. (The scattering cross section σ_{scat} takes account of a nuclear and long-range interaction.) E_{min} is the minimum energy of atoms after colliding with which a neutron is able to escape the trap $E_{\text{min}} = E_{\text{UCN}}^{\text{trap}} (M+1)^2 / 4M$, and ε_{min} is minimum recoil energy when UCNs escape from the trap. To simplify, the UCN initial energy is equal to zero, $\varepsilon_{\text{min}} = E_{\text{UCN}}^{\text{trap}}$, and

$E_A 4M/(M+1)^2$ is the maximum neutron recoil energy. The flux of atoms is

$$d\Phi(E_A)/dE_A = \frac{n_A \bar{V}_A}{(kT)^2} E_A \exp\left\{-\frac{E_A}{kT}\right\}, \quad (14)$$

where n_A is the number of atoms (in cm^{-3}) at temperature T , \bar{V}_A is the average velocity of atoms of mass $m_n M$ at temperature T , and $\bar{V}_A = 4(kT/2\pi m_n M)^{1/2}$. The gas density n_A (cm^{-3}) = $2.687 \times 10^{16} \times P_A$ (mbar) $\times 273/T$ (K), where P_A is an experimentally measured gas pressure.

We can rewrite formula (13) in the following way:

$$\begin{aligned} & (\tau_{\text{stor}}^{\text{gas}} n_A \bar{V}_A)^{-1} - \sigma_{\text{capt}}^0 \bar{V}_{2200}/\bar{V}_A \\ &= \frac{\pi(M+1)^2}{M} b_{\text{free-nucl}}^2 \int_{E_{\text{UCN}}^{\text{trap}} \frac{(M+1)^2}{4M}}^{\infty} dE_A \int_{E_{\text{UCN}}^{\text{trap}}}^{E_A \frac{4M}{(M+1)^2}} \\ & \times \frac{E_A}{(kT)^2} e^{-E_A/kT} \left[1 \pm \frac{g_{\pm}^2 M^2}{\pi(M+1)} \frac{m_n c^2}{b_{\text{free-nucl}} \hbar c} \right. \\ & \times \frac{\lambda^2}{2m_n \varepsilon \lambda^2 / \hbar^2 + 1} + \frac{(g_{\pm}^2 M)^2}{(M+1)^2} \\ & \left. \times \left(\frac{m_n c}{2\pi \hbar b_{\text{free-nucl}}} \right)^2 \frac{\lambda^4}{(2m_n \lambda^2 \varepsilon / \hbar^2 + 1)^2} \right] \frac{d\varepsilon}{E_A}. \quad (15) \end{aligned}$$

After integration one can subtract the contribution made by long-range forces as follows:

$$\begin{aligned} & \Delta_1^{P\tau \text{ nucl}} \\ &= \left[\frac{(\tau_{\text{stor}}^{\text{gas}} n_A \bar{V}_A)^{-1} - \sigma_{\text{capt}}^0 \bar{V}_{2200}/\bar{V}_A e^{\frac{E_{\text{UCN}}^{\text{trap}} (M+1)^2}{kT}}}{4\pi b_{\text{free-nucl}}^2} - 1 \right] \\ &= \pm \frac{g_{\pm}^2 M(M+1)}{8\pi b_{\text{free-nucl}}} \left(\frac{\hbar c}{kT} \right) e^{z(\lambda)} E_1[z(\lambda)] \\ &+ \frac{g_{\pm}^4}{4} \frac{M^2(M+1)^2}{(8\pi b_{\text{free-nucl}})^2} \left(\frac{\hbar c}{kT} \right)^2 \frac{e^{z(\lambda)} E_2[z(\lambda)]}{z}, \quad (16) \end{aligned}$$

where $E_1(z)$ and $E_2(z)$ are exponential integrals. The value $z(\lambda) \equiv \frac{(M+1)^2}{4M} \left(\frac{\hbar^2}{2m_n k T \lambda^2} + \frac{E_{\text{UCN}}^{\text{trap}}}{kT} \right)$ is a function of a few variables: M , λ , and T .

The expression in the square brackets following the first equals in formula (16) is an expected experimental effect resulting from the long-range interaction. It is defined as $\Delta_1^{P\tau \text{ nucl}}$ since in this analysis we compare the nuclear scattering cross section and the scattering cross section obtained from $(P\tau)$ measurements with UCNs. We assume that information on the nuclear scattering cross section ($4\pi b_{\text{free-nucl}}^2$) is available. In fact, this information can be obtained from a neutron-scattering experiment at a neutron energy of about 1 eV because at large recoil momentum the contribution from a long-range interaction is negligible.

Let us calculate the value of an expected experimental effect $\Delta_1^{P\tau \text{ nucl}}$ depending on g^2 and λ . The case of a repulsive potential (a vector boson) and the case of an attractive potential (a scalar boson) significantly differ by the effect shape. In the

case of a vector boson the effect is positive for any g^2 and λ . For a scalar boson the effect can change sign depending on g^2 and λ . The shape of a possible effect for both cases is shown in Figs. 3(a) and 3(c). Figures 3(b) and 3(d) show the correlation between g^2 and λ , which arises when this surface is crossed by the planes $\Delta_1^{P\tau \text{ nucl}} = \pm 0.3$, $\Delta_1^{P\tau \text{ nucl}} = \pm 0.03$, and $\Delta_1^{P\tau \text{ nucl}} = \pm 0.003$. In the case when $\varphi > 0$, the value $\Delta_1^{P\tau \text{ nucl}}$ can be only positive. In the case when $\varphi < 0$, $\Delta_1^{P\tau \text{ nucl}}$ can have any sign. Therefore at $\Delta_1^{P\tau \text{ nucl}} > 0$ the determination of a potential sign from an experiment is ambiguous. As a rule we are compelled to analyze both cases: $\varphi > 0$ and $\varphi < 0$.

As seen from Fig. 3 the method of comparing the scattering cross section of UCNs and the nuclear scattering cross section becomes insensitive in the area of 10^{-8} – 10^{-4} cm. This is due to a slightly increasing logarithmic dependence in (8) at sufficiently high energy of incident atoms at room temperature (lowering the temperature of the gas may result in some progress). Thus, the integral measurement method of UCNs essentially determines the scattering cross section in the field of forces less than 10^{-8} cm ($\lambda < 10^{-8}$ cm). The method of measuring low-energy neutrons is sensitive down to $\lambda \approx \lambda_{\text{UCN}}$, i.e., 10^{-6} cm ($\lambda_{\text{UCN}}^2 = \hbar^2/2m_n E_{\text{UCN}}^{\text{trap}}$). [In formula (9) under the logarithm there is the squared ratio of λ to λ_{UCN} .] To identify long-range forces at $\lambda > 10^{-6}$ cm, one should compare the scattering cross section of UCNs with the value of $4\pi b_{\text{free-int}}^2$, where $b_{\text{free-int}}$ is a scattering length measured by a neutron interferometer: $b_{\text{free-int}} = b_{\text{free-nucl}} + b_{\text{long-range}}$. The method using the scattering length measured by a neutron interferometer will probably be more insensitive (by a few centimeters) in the area of λ than the coherence length of the neutron beam in measurements by interferometers.

Recently, we realized the preliminary measurements of $P\tau$ for He with an accuracy of about 1% [$P\tau = (427 \pm 4)$ mbr s]. Results of our measurements are in agreement with results of the similar measurements published in Ref. [25] [$P\tau = (467 \pm 33)$ mbr s].

Using the obtained value of $P\tau$, we can express the total cross section with the formula $\sigma_{\text{scat}}^{\text{He}} + \sigma_{\text{He-capt}}^0 \bar{V}_{2200}/\bar{V}_{\text{He}} = (n_{\text{He}} \bar{V}_{\text{He}} \tau_{\text{stor}}^{\text{gas}})^{-1} = (P\tau_{\text{stor}}^{\text{gas}} \times 2.687 \times 10^{16} \times 273/293 \bar{V}_{\text{He}})^{-1}$, where 2.687×10^{16} is the number of helium atoms in 1 cm^3 at a pressure of 1 mbar and temperature $T = 273$ K, \bar{V}_{He} is the average velocity of helium atoms at room temperature (293 K), $\bar{V}_{\text{He}} = 1.240 \times 10^5 \text{ cm s}^{-1}$, and $P\tau = (427 \pm 4)$ mbr s. Then $\sigma_{\text{scat}}^{\text{He}} + \sigma_{\text{He-capt}}^0 \bar{V}_{2200}/\bar{V}_{\text{He}} = (0.753 \pm 0.006) \times 10^{-24} \text{ cm}^2$. The capture cross section of natural He because of an admixture of He^3 is equal to $0.0075 \times 10^{-24} \text{ cm}^2$ for a velocity of 2200 m/s; correspondingly, the capture cross section for the average velocity $1.240 \times 10^5 \text{ cm s}^{-1}$ is equal to $0.0133 \times 10^{-24} \text{ cm}^2$. Then the scattering cross section $\sigma_{\text{scat}}^{\text{He}}(\text{exp. } P\tau) = (0.740 \pm 0.006) \times 10^{-24} \text{ cm}^2$.

The nuclear scattering cross section $\sigma_{\text{free-nucl}}^{\text{He}}$ measured by the transmission of neutrons with energy from 0.19 up to 6.19 eV through a volume with He gas [26] gives $0.773 \pm 0.009 \times 10^{-24} \text{ cm}^2$. The measurements carried out before [27] give $0.73 \pm 0.05 \times 10^{-24} \text{ cm}^2$. In the tables of the neutron cross-section data [28] the recommended average

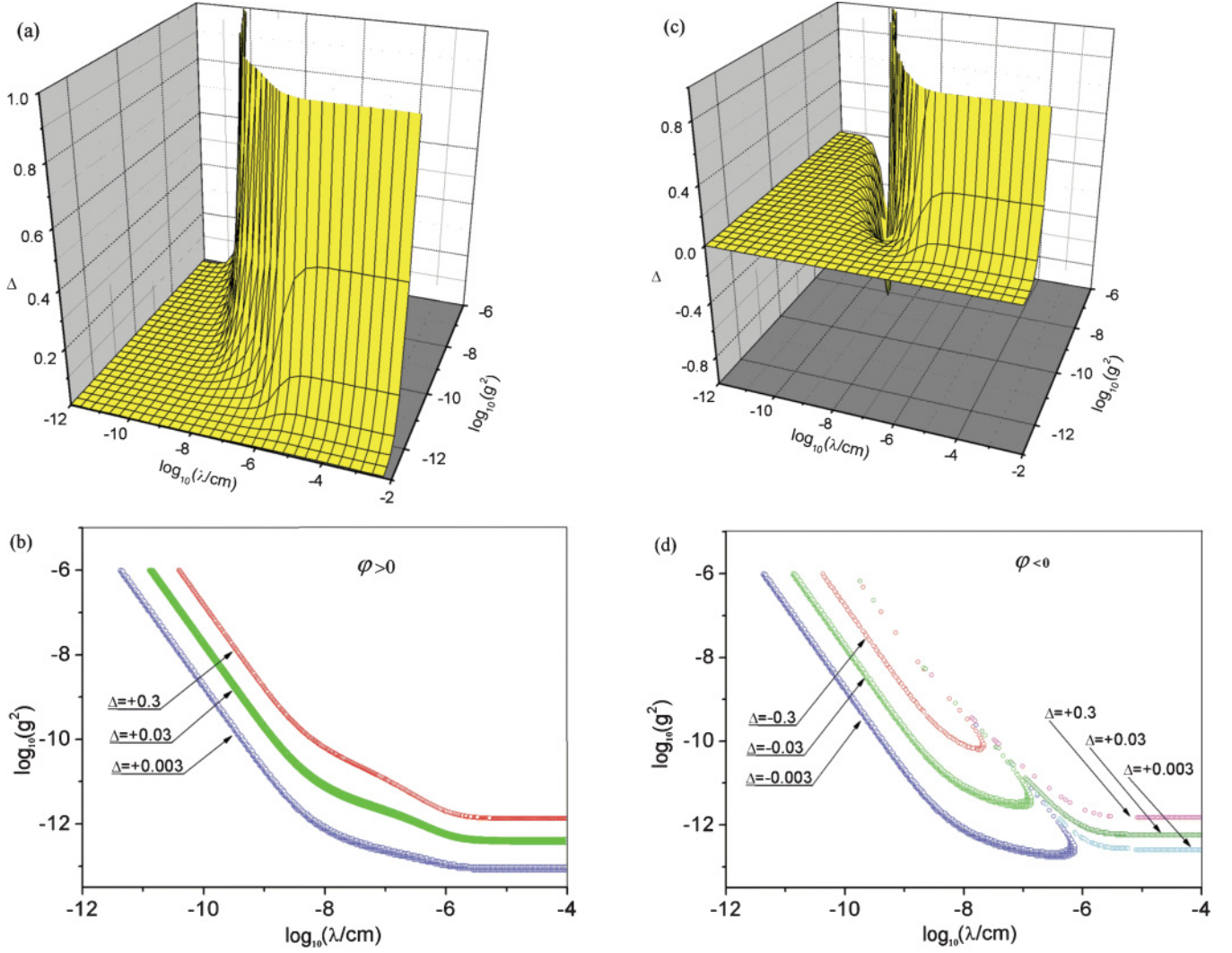


FIG. 3. (Color online) Dependence of an expected experimental effect $\Delta_1^{P\tau \text{ nucl}}$ on parameters g^2 and λ for He. (a) The case of a repulsive potential, i.e., an exchange by a vector boson. (b) Correlation between parameters g^2 and λ for a repulsive potential if the effect $\Delta_1^{P\tau \text{ nucl}}$ is equal to 0.3, 0.03, and 0.003. (c) The case of an attractive potential, i.e., an exchange by a scalar boson. (d) Correlation between parameters g^2 and λ for an attractive potential if the effect $\Delta_1^{P\tau \text{ nucl}}$ is equal to ± 0.3 , ± 0.03 , and ± 0.003 .

value of $0.76 \pm 0.01 \times 10^{-24} \text{ cm}^2$ is presented. Using this value, we obtain the following $\Delta_1^{P\tau \text{ nucl}}$ value:

$$\Delta_{1,\text{He}}^{P\tau \text{ nucl}} = \left[\frac{\sigma_{\text{scat}}^{\text{He}} (\exp \cdot P\tau) e^{\frac{E_{\text{UCN}}^{\text{trap}} (M+1)^2}{kT}}}{\sigma_{\text{free-nucl}}^{\text{He}}} - 1 \right] = -0.026 \pm 0.015(1.7\sigma).$$

We do not see any real effect, and for simplicity we can estimate the upper limit for $\Delta_{1,\text{He}}^{P\tau \text{ nucl}}$ as +0.03 or as -0.03 at a confidence level of 95% (2σ). In Fig. 4 the restriction area (g^2, λ) at a confidence level of 95% is shown

for the case of an attractive potential and for a repulsive potential.

Now it is necessary to compare the nuclear scattering cross section measured by means of the $P\tau$ method and the coherent scattering cross section measured by means of interferometers. The measurements of scattering lengths by means of interferometers $b_{\text{free-int}}$ should also include the scattering length of long-range interaction ($b_{\text{free-int}} = b_{\text{free-nucl}} + b_{\text{long-range}}$) since the scattering length is measured at zero scattering angle, i.e., $4\pi b_{\text{free-int}}^2 = 4\pi (b_{\text{free-nucl}} + b_{\text{long-range}})^2$. Therefore we can obtain the following formula:

$$\Delta_2^{P\tau \text{ int}} = \left[\frac{(\tau_{\text{stor}}^{\text{gas}} n_A \bar{V}_A)^{-1} - \sigma_{\text{capt}}^0 V_{2200} / \bar{V}_A e^{\frac{E_{\text{UCN}}^{\text{trap}} (M+1)^2}{kT}}}{4\pi b_{\text{free-int}}^2} - 1 \right] = \pm g_{\pm}^2 M \left\{ \frac{(M+1)}{8\pi b_{\text{free-int}}} \left(\frac{\hbar c}{kT} \right) e^{z(\lambda)} E_1[z(\lambda)] - \left(\frac{M}{M+1} \right) \frac{\lambda^2}{\pi b_{\text{free-int}}} \frac{m_n c}{\hbar} \right\}$$

$$\begin{aligned}
& + (g_{\pm}^2 M)^2 \left\{ \frac{(M+1)^2}{4(8\pi b_{\text{free-int}})^2} \left(\frac{\hbar c}{kT} \right)^2 \frac{e^{z(\lambda)} E_2[z(\lambda)]}{z} + \left(\frac{M}{M+1} \right)^2 \left(\frac{m_n c \lambda^2}{2\pi \hbar b_{\text{free-int}}} \right)^2 \right. \\
& \left. - \left(\frac{m_n c M \lambda^2}{16\pi^2 \hbar b_{\text{free-int}}^2} \right) \left(\frac{\hbar c}{kT} \right) e^{z(\lambda)} E_1[z(\lambda)] \right\} \approx \left[1 \mp \frac{1}{2} J_0(g_{\pm}^2, \lambda) \right]^2 - 1, \quad (17)
\end{aligned}$$

where $J_0(g_{\pm}^2, \lambda) = \frac{g_{\pm}^2 M^2}{\pi(M+1)} \frac{\lambda^2}{b_{\text{free-int}} \lambda_C}$ and λ_C is the Compton neutron wave length, $\lambda_C = \frac{\hbar}{m_n c}$.

The analysis using the simplified formula (17) for $\Delta_2^{P\tau \text{ int}}$ and for $\lambda > 10^{-7} \text{cm}$ is also shown in Fig. 4. The value $b_{\text{bound-int}}$ was taken from Ref. [30] ($b_{\text{bound-int, He}} = 3.26 \pm 0.03 \text{fm}$). Since in our case one discusses scattering with a free nucleus, we should recalculate the scattering length for bound He nucleus in regard to the scattering length with a free nucleus of helium using the equation $b_{\text{free-nucl, He}} = b_{\text{bound-nucl, He}} M_{\text{He}} / (M_{\text{He}} + 1) = 0.2608(24) \times 10^{-12} \text{cm}$. Accordingly, the cross sections with a free nucleus, calculated from the scattering length with a free nucleus, will be $\sigma_0^{\text{He}} = 4\pi b_{\text{free-nucl, He}}^2 = 0.855(16) \times 10^{-24} \text{cm}^2$. At the same time the scattering cross section $\sigma_{\text{scat}}^{\text{He}}(\text{exp. } P\tau) = (0.740 \pm 0.006) \times 10^{-24} \text{cm}^2$. Then

$$\begin{aligned}
\Delta_{2, \text{He}}^{P\tau \text{ int}} &= \left[\frac{\sigma_{\text{scat}}^{\text{He}}(\text{exp. } P\tau) e^{\frac{E_{\text{UCN}}^{\text{trap}} (M+1)^2}{kT}}}{4\pi b_{\text{free-int, He}}^2} - 1 \right] \\
&= -0.134 \pm 0.018(7.5\sigma).
\end{aligned}$$

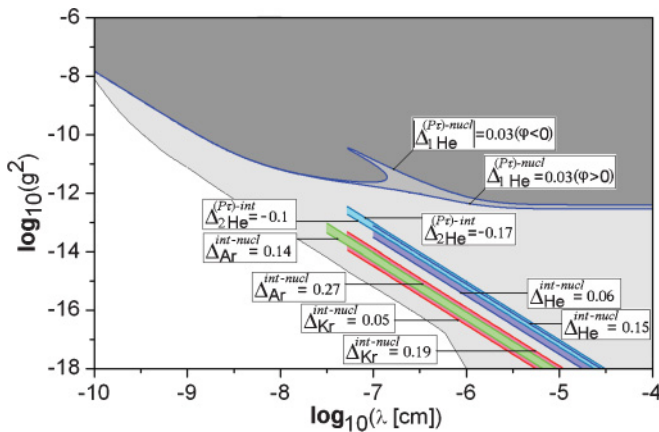


FIG. 4. (Color online) The dark shaded area corresponds to constraints for g^2 and λ from our preliminary measurements of the $P\tau$ value for He [$P\tau = (427 \pm 4) \text{mbrs}$] and the nuclear scattering cross section $\sigma_{\text{free-nucl}}^{\text{He}}$ ($0.76 \pm 0.01 \times 10^{-24} \text{cm}^2$) measured by the neutron transmission [26–28]. The light shaded area corresponds to constraints for g^2 and λ from Refs. [9,10]. The upper inclined area $\Delta_{2, \text{He}}^{P\tau \text{ int}}$ corresponds to values of g^2 and λ from a comparison of the $P\tau$ method for He [$P\tau = (427 \pm 4) \text{mbrs}$] and the interferometer method [29] for He. The other inclined areas $\Delta_{\text{He}}^{\text{int-nucl}}$, $\Delta_{\text{Ar}}^{\text{int-nucl}}$, and $\Delta_{\text{Kr}}^{\text{int-nucl}}$ correspond to values of g^2 and λ from a comparison of the scattering cross sections measured by the transmission method [26] and by mean interferometer [29] for He, Ar, and Kr. For all cases $\Delta_{2, \text{He}}^{P\tau \text{ int}}$, $\Delta_{\text{He}}^{\text{int-nucl}}$, $\Delta_{\text{Ar}}^{\text{int-nucl}}$, and $\Delta_{\text{Kr}}^{\text{int-nucl}}$ the solution exists only for repulsive potential.

At a confidence level of 95% (2σ) the effect lies in the range $(-0.17, -0.1)$. The area (g^2, λ) is shown in Fig. 4 at a confidence level of 95% for the case of a repulsive potential. There is no solution for an attractive potential. One can see that the determined area of values of g^2 and λ are excluded by analysis results [9,10].

It would be very interesting to have now precise $P\tau$ data for the heavy atoms. But this is not measured yet; therefore we will use the scattering cross sections measured by the transmission of the collimated neutron beam with different energies (from 0.07 up to 6 eV) through the sample with the studied gas [26]. We can compare these cross sections with the cross sections measured by means of an interferometer [29] for the same gases. Making the comparison, we have to take into account the correction for incoherent scattering cross section, and we have to recalculate the bound cross section to the scattering cross section on the free atom. The results of the comparison are shown in Table I. One can see that the values measured by the transmission method, except for the neon case, are less than similar values obtained from neutron interferometer data.

The analysis of the effect of the long-range forces can be done by using the following formula:

$$\begin{aligned}
\Delta^{\text{int-nucl}} &= \frac{\sigma_{\text{coh-free}}^{**}}{\sigma_{\text{coh-free}}^*} - 1 \\
&= \frac{1}{4} \left[\frac{g_{\pm}^2 M^2}{\pi(M+1)} \right]^2 \left(\frac{\lambda^2}{b_{\text{free-nucl}} \lambda_C} \right)^2 \\
&\quad \pm \frac{g_{\pm}^2 M^2}{\pi(M+1)} \frac{\lambda^2}{b_{\text{free-nucl}} \lambda_C}, \quad (18)
\end{aligned}$$

where the coherent cross sections $\sigma_{\text{coh-free}}^*$ measured with the transmission method is $\sigma_{\text{coh-free}}^* = \sigma_{\text{scat-free}} - \sigma_{\text{inc-free}}$. The total scattering cross section $\sigma_{\text{scat-free}}$ was taken from Ref. [26].

The incoherent scattering cross section $\sigma_{\text{inc-free}} = [M/(M+1)]^2 \sigma_{\text{inc}}$, and the bound incoherent cross section σ_{inc}^* is taken from Ref. [31]. $\sigma_{\text{coh-free}}^{**} = 4\pi [M/(M+1)]^2 b_c^2$, where b_c is taken from Ref. [29]. $b_{\text{free-nucl}} = \sqrt{\sigma_{\text{coh-free}}^*/4\pi}$.

The result of this analysis is presented in Fig. 4 at a confidence level of 95% (2σ). One can see that the determined area of g^2 and λ is excluded from analysis results [9,10]. The difference between the results of the transmission method and neutron interferometer measurements cannot be explained by the $n-e$ scattering because the $n-e$ scattering length is much smaller than the experimental discrepancy.

The presented discrepancy is likely to be due to a systematic experimental error. To clarify the problem new measurements are to be made for $P\tau$ data, but it is also important to test the measurement of scattering lengths by means of the interferometer. Finally, if there is some chance that the observed

TABLE I. The coherent cross sections $\sigma_{\text{coh-free}}^*$ measured by the transmission method [26] and the coherent cross sections $\sigma_{\text{coh-free}}^{**}$ measured by the neutron interferometer [29].

Gas	Transmission method $\sigma_{\text{coh-free}}^*$ (10^{-24} cm ²)	Neutron interferometer $\sigma_{\text{coh-free}}^{**}$ (10^{-24} cm ²)	$\Delta\sigma = \sigma_{\text{coh-free}}^* - \sigma_{\text{coh-free}}^{**}$
He	0.773 ± 0.009	0.855 ± 0.016	$-0.082 \pm 0.018(4.5\sigma)$
Ne	2.42 ± 0.03	2.44 ± 0.04	$-0.02 \pm 0.05(0.4\sigma)$
Ar	0.424 ± 0.008	0.51 ± 0.01	$-0.086 \pm 0.012(7\sigma)$
Kr	6.19 ± 0.17	6.94 ± 0.11	$-0.75 \pm 0.20(4\sigma)$

difference is caused by long-range forces, it could be tested by using the method of measuring the flux of above-barrier neutrons. This method is sensitive to the long-range forces also.

The method of measuring the flux of above-barrier neutrons will be considered in the next section.

V. THE METHOD OF MEASURING THE FLUX OF ABOVE-BARRIER NEUTRONS

If there is no gas in the trap, the number of neutrons up scattered within an energy range from the critical energy of the foil $E_{\text{UCN}}^{\text{foil}}$ to that of the trap $E_{\text{UCN}}^{\text{trap}}$ is determined by UCN collision with the trap walls and is equal to

$$\begin{aligned} N_{\text{low}}(0) &= \int_0^\infty N_0(0) e^{-t/\tau_{\text{stor}}^{\text{total}}(n_A=0)} \alpha \nu dt \\ &= N_0(0) \alpha \nu \tau_{\text{stor}}^{\text{total}}(n_A=0), \end{aligned} \quad (19)$$

where α is the probability per one collision that UCN will be up scattered within the range $E_{\text{UCN}}^{\text{foil}}$ to $E_{\text{UCN}}^{\text{trap}}$, ν is frequency of UCN collision with the trap walls, $\tau_{\text{stor}}^{\text{total}}(n_A=0)$ is UCN storage time without gas, and $N_0(0)$ is the number of UCNs in the trap without gas at the moment of the beginning of the lower up-scattering effect measurements.

When a gas at density n_A is available, the number of neutrons up scattered within the same energy range will be equal to

$$\begin{aligned} N_{\text{low}}(n_A) &= \int_0^\infty e^{-t/\tau_{\text{stor}}^{\text{total}}(n_A)} N_0(n_A) [\alpha \nu + W_{\text{at}}^{\text{low}}(n_A)] dt \\ &= N_0(n_A) [\alpha \nu + W_{\text{at}}^{\text{low}}(n_A)] \tau_{\text{stor}}^{\text{total}}(n_A), \end{aligned} \quad (20)$$

where $W_{\text{at}}^{\text{low}}(n_A)$ is the probability that UCNs will be up scattered within the range $E_{\text{UCN}}^{\text{foil}}$ to $E_{\text{UCN}}^{\text{trap}}$, $\tau_{\text{stor}}^{\text{total}}(n_A)$ is the storage time of UCNs in the trap with the available gas at density n_A , and $N_0(n_A)$ is the total number of UCNs in the trap with the gas at the moment of the beginning of measuring the lower-energy up-scattering effect.

Combining Eqs. (19) and (20), one can obtain the following equation for subtraction of $W_{\text{at}}^{\text{low}}(n_A)$ from the experiment:

$$W_{\text{at}}^{\text{low}}(n_A) = \frac{N_{\text{low}}(n_A)}{N_0(n_A) \tau_{\text{tot.st}}^{\text{up}}(n_A)} - \frac{N_{\text{low}}(0)}{N_0(0) \tau_{\text{tot.st}}^{\text{up}}(0)}. \quad (21)$$

Let us calculate $W_{\text{at}}^{\text{low}}(n_A)$, taking into account the effect of long-range forces.

$$\begin{aligned} W_{\text{at}}^{\text{low}}(n_A) &= \int_{\varepsilon_f}^{\varepsilon_t} d\sigma(\varepsilon) \int_{\varepsilon}^{\varepsilon} \frac{(M+1)^2}{4M} d\Phi(E_A) \\ &= \pi \frac{(M+1)^2}{M} n_A b_{\text{free-nucl}}^2 \left(\frac{\bar{V}_A}{kT} \right) \int_{\varepsilon_f}^{\varepsilon_t} e^{-\varepsilon \frac{(M+1)^2}{4M} / kT} \end{aligned}$$

$$\begin{aligned} &\times \left[1 \pm \frac{g_{\pm}^2 M^2}{\pi(M+1) b_{\text{free-nucl}} \hbar} \frac{m_n c}{2m_n \varepsilon \lambda^2 / \hbar^2 + 1} \right. \\ &+ (g_{\pm}^2 M)^2 \frac{M^2}{(M+1)^2} \left(\frac{m_n c}{2\pi \hbar b_{\text{free-nucl}}} \right)^2 \\ &\left. \times \frac{\lambda^4}{(2m_n \lambda^2 \varepsilon / \hbar^2 + 1)^2} \right] d\varepsilon. \end{aligned} \quad (22)$$

In calculating integral (22) we assume ε_t and ε_f to have the same order of magnitude; therefore a variable ε is replaced by its average value of integration interval $\bar{\varepsilon} = (\varepsilon_t + \varepsilon_f)/2$. Now we can subtract the contribution made by nuclear scattering and obtain the following equation for g_{\pm}^2 and λ :

$$\begin{aligned} W_{\text{at}}^{\text{low}}(n_A) / n_A \bar{V}_A \frac{(\varepsilon_t - \varepsilon_f)}{kT} 4\pi b_{\text{free-nucl}}^2 \frac{(M+1)^2}{M} \\ = \frac{1}{4} \left[1 \pm \frac{1}{2} J_1(g_{\pm}^2, \lambda) \right]^2, \end{aligned} \quad (23)$$

where

$$J_1(g_{\pm}^2, \lambda) = \frac{g_{\pm}^2 M^2}{\pi(M+1) b_{\text{free-nucl}} \bar{\lambda}_C} \frac{1}{\lambda^2 / \bar{\lambda}_{\text{UCN}}^2 + 1}. \quad (24)$$

Here $\bar{\lambda}_{\text{UCN}}$ is the de Broglie wave length ($\bar{\lambda}_{\text{UCN}}^2 = \hbar^2 / 2m_n \bar{\varepsilon}$) of the neutron with kinetic energy $\bar{\varepsilon} = (\varepsilon_t + \varepsilon_f)/2$.

The left part of Eq. (23) implies $W_{\text{at}}^{\text{low}}(n_A)$ determined from the experiment according to Eq. (21). This equation contains the ratio of the counting rate of neutrons at the energy above $E_{\text{UCN}}^{\text{foil}}$ to that of neutrons at the energy below $E_{\text{UCN}}^{\text{foil}}$. The counting efficiency of neutrons depends on energy; thus achieving a very high accuracy of $W_{\text{at}}^{\text{low}}(n_A)$ is a particular problem. This problem can be solved using the method of relative measurements. For this purpose it is necessary to take the ratio of Eq. (23), for example, for ^{86}Kr and He

$$\begin{aligned} &\frac{[W_{\text{at}}^{\text{low}}(n_A) / n_A \bar{V}_A \frac{(\varepsilon_t - \varepsilon_f)}{kT} 4\pi b_{\text{free-nucl}}^2 \frac{(M+1)^2}{M}]_{\text{Kr}}}{[W_{\text{at}}^{\text{low}}(n_A) / n_A \bar{V}_A \frac{(\varepsilon_t - \varepsilon_f)}{kT} 4\pi b_{\text{free-nucl}}^2 \frac{(M+1)^2}{M}]_{\text{He}}} \\ &\approx \left\{ 1 \pm \left[\frac{M_{\text{Kr}}^2}{(M+1)_{\text{Kr}} b_{\text{free-nucl}}^{\text{Kr}}} - \frac{M_{\text{He}}^2}{(M+1)_{\text{He}} b_{\text{free-nucl}}^{\text{He}}} \right] \right. \\ &\left. \times \frac{g_{\pm}^2}{2\pi \bar{\lambda}_C} \frac{\lambda^2}{\lambda^2 / \bar{\lambda}_{\text{UCN}}^2 + 1} \right\}^2. \end{aligned} \quad (25)$$

In this ratio efficiencies of the detector are cancelled, and the correction in the right part for He is much less than for ^{86}Kr . From this formula one can see that for $\lambda > \bar{\lambda}_{\text{UCN}}$ the method sensitivity comes to saturation. In a similar way we can get the

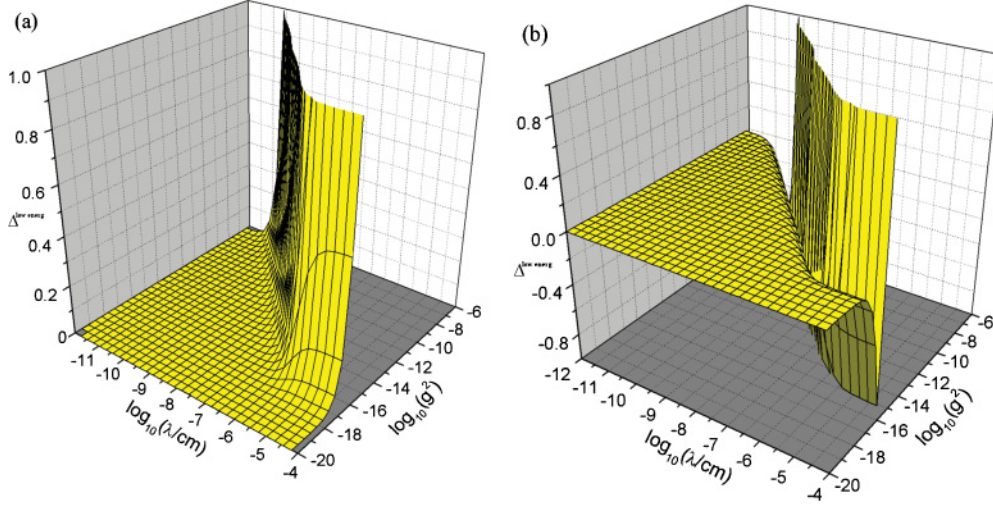


FIG. 5. (Color online) Dependence of $\Delta_3^{\text{low-energ-nucl}}$ on g^2 and λ : (a) for $\varphi > 0$ and (b) for $\varphi < 0$.

value of $\Delta_3^{\text{low-energ-nucl}}$:

$$\Delta_3^{\text{low-energ-nucl}} = \frac{[W_{\text{at}}^{\text{low}}(n_A)/n_A \bar{V}_A \frac{(\varepsilon_i - \varepsilon_f)}{kT} 4\pi b_{\text{free-nucl}}^2 \frac{(M+1)^2}{M}]_{\text{Kr}}}{[W_{\text{at}}^{\text{low}}(n_A)/n_A \bar{V}_A \frac{(\varepsilon_i - \varepsilon_f)}{kT} 4\pi b_{\text{free-nucl}}^2 \frac{(M+1)^2}{M}]_{\text{He}}} - 1. \quad (26)$$

In Figs. 5(a) and 5(b) the values of the possible effect of $\Delta_3^{\text{low-energ-nucl}}$ are presented in the form of a surface for cases of positive and negative potentials φ .

Now we would like to make an analysis using the coherence neutron-scattering length $b_{\text{free-int}}$ derived from interferometer measurements. In this case we can obtain the following formula:

$$\begin{aligned} & \frac{[W_{\text{at}}^{\text{low}}(n_A)/n_A \bar{V}_A \frac{(\varepsilon_i - \varepsilon_f)}{kT} 4\pi b_{\text{free-int}}^2 \frac{(M+1)^2}{M}]_{\text{Kr}}}{[W_{\text{at}}^{\text{low}}(n_A)/n_A \bar{V}_A \frac{(\varepsilon_i - \varepsilon_f)}{kT} 4\pi b_{\text{free-int}}^2 \frac{(M+1)^2}{M}]_{\text{He}}} \\ & \approx \left\{ 1 \mp \left[\frac{M_{\text{Kr}}^2}{(M+1)_{\text{Kr}} b_{\text{free-int}}^{\text{Kr}}} - \frac{M_{\text{He}}^2}{(M+1)_{\text{He}} b_{\text{free-int}}^{\text{He}}} \right] \right. \\ & \quad \left. \times \frac{g_{\pm}^2 \lambda^2}{2\pi \bar{\lambda}_C} \left(\frac{\lambda^2}{\bar{\lambda}_{\text{UCN}}^2} \right) \frac{1}{\lambda^2 / \bar{\lambda}_{\text{UCN}}^2 + 1} \right\}^2. \quad (27) \end{aligned}$$

Again, we can introduce $\Delta_4^{\text{low-energ-int}}$:

$$\Delta_4^{\text{low-energ-int}} = \frac{[W_{\text{at}}^{\text{low}}(n_A)/n_A \bar{V}_A \frac{(\varepsilon_i - \varepsilon_f)}{kT} 4\pi b_{\text{free-int}}^2 \frac{(M+1)^2}{M}]_{\text{Kr}}}{[W_{\text{at}}^{\text{low}}(n_A)/n_A \bar{V}_A \frac{(\varepsilon_i - \varepsilon_f)}{kT} 4\pi b_{\text{free-int}}^2 \frac{(M+1)^2}{M}]_{\text{He}}} - 1. \quad (28)$$

In this case the method becomes sensitive for $\lambda > \bar{\lambda}_{\text{UCN}}$.

Now let us compare the $P\tau$ method and that of above-barrier neutrons for two cases of analysis: with $b = b_{\text{free-nucl}}$ and with $b = b_{\text{free-int}}$. These results are shown in Figs. 6(a)–6(d). We have to keep in mind that (i) $\Delta_1^{P\tau \text{ nucl}}$ is the $P\tau$

measurement of the scattering cross section in comparison with the nuclear scattering cross section measured at a neutron energy about 1 eV, (ii) $\Delta_2^{P\tau \text{ int}}$ is the $P\tau$ measurement of the scattering cross section in comparison with $4\pi b_{\text{free-int}}^2$ measured by means of a neutron interferometer, (iii) $\Delta_3^{\text{low-energ-nucl}}$ is the method of above-barrier neutrons in comparison with the nuclear scattering cross section measured at a neutron energy of about 1 eV, and (iv) $\Delta_4^{\text{low-energ-int}}$ is the method of above-barrier neutrons in comparison with $b_{\text{free-int}}$ measured by means of a neutron interferometer.

If one assume that Δ is determined at an accuracy of about 1% (for a confidence level of 95%, the upper limit of Δ is about +0.03 or –0.03). The dependence of g^2 on λ will look like, for example, for krypton-86, as shown in Figs. 6(a)–6(d). The analysis is made for the case of $\varphi > 0$ [Figs. 6(a) and 6(c)] and for the case of $\varphi < 0$ [Figs. 6(b) and 6(d)]. One can see that the independence of g^2 from λ is already observed within the area 10^{-8} – 10^{-4} cm for $\Delta_1^{P\tau \text{ nucl}}$, but for $\Delta_3^{\text{low-energ-nucl}}$ the independence of g^2 from λ is within the area 10^{-6} – 10^{-4} cm. For $\Delta_2^{P\tau \text{ int}}$ and $\Delta_4^{\text{low-energ-int}}$ the independence of g^2 from λ will take place within the area of λ exceeding the length of neutron beam coherence in measurements with interferometers by a few centimeters.

Now we would like to discuss some details of the experiment on above-barrier neutrons. It is necessary to take into account that values N_{low} and N_0 in Eqs. (19)–(21) are different from the detector counting rate N_{low}^* and N_0^* . The probability of detection of a neutron is determined by the ratio of probability of neutron leakage to the detector τ_{emp}^{-1} to the total probability of UCN losses $\tau_{\text{emp}}^{-1} + \tau_{\text{stor}}^{-1}$, i.e., by the ratio $\frac{\tau_{\text{emp}}^{-1}}{\tau_{\text{emp}}^{-1} + \tau_{\text{stor}}^{-1}}$, where τ_{emp} is the time of UCNs leaving the trap and τ_{stor} is the UCN storage time in the trap. In addition, it is necessary to take into account the efficiency of the detector D_{up} for the corresponding energy range and also the transmission foil factor T_{foil} .

Thus, the number of neutrons N_{low} at an energy above $E_{\text{UCN}}^{\text{foil}}$ but below $E_{\text{UCN}}^{\text{trap}}$ is connected to the counting rate of the

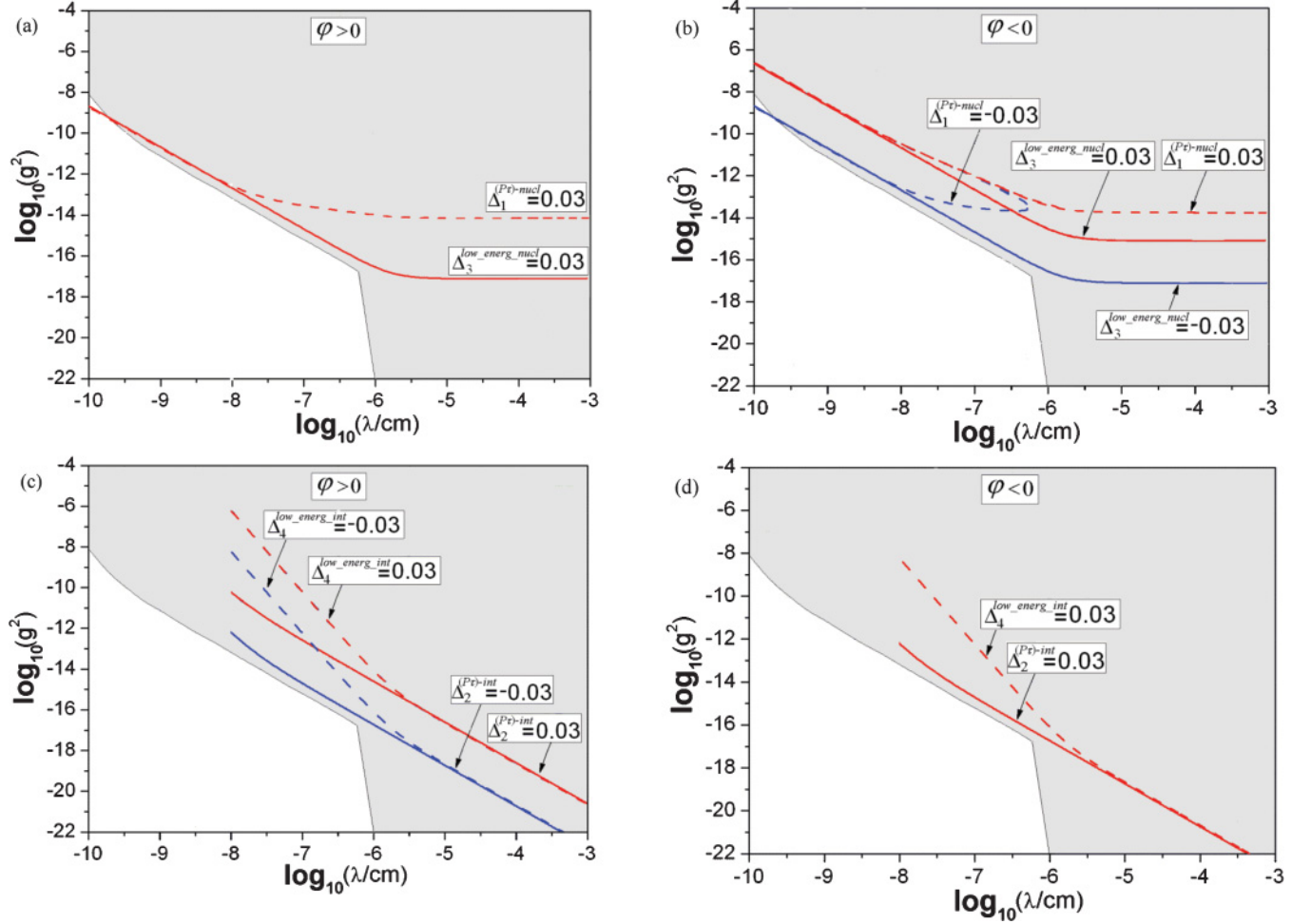


FIG. 6. (Color online) The comparison of the constrains (95% C.L.) from the $(P\tau)$ method and the method of above-barrier neutrons for two cases of analysis: with $b = b_{\text{free-nucl}}$ and with $b = b_{\text{free-int}}$ for the case of ^{86}Kr . (a) $\varphi > 0$, $\Delta_1^{P\tau\text{-nucl}} = 0.03$, $\Delta_3^{\text{low-energ-nucl}} = 0.03$; (b) $\varphi < 0$, $\Delta_1^{P\tau\text{-nucl}} = 0.03$ or -0.03 , $\Delta_3^{\text{low-energ-nucl}} = 0.03$ or -0.03 ; (c) $\varphi > 0$, $\Delta_2^{P\tau\text{-int}} = 0.03$ or -0.03 , $\Delta_4^{\text{low-energ-int}} = 0.03$ or -0.03 ; (d) $\varphi < 0$, $\Delta_2^{P\tau\text{-int}} = 0.03$, $\Delta_4^{\text{low-energ-int}} = 0.03$. The shaded area shows excluded values of g^2 and λ from Refs. [9,10].

detector N_{low}^* by the following relation:

$$N_{\text{low}}(n_A) = \frac{N_{\text{low}}^*(n_A)}{d_{\text{up}}(n_A)}, \quad (29)$$

where $d_{\text{up}}(n_A) = T_{\text{foil}} D_{\text{up}} \tau_{\text{stor}}^{\text{up}}(n_A) / [\tau_{\text{stor}}^{\text{up}}(n_A) + \tau_{\text{emp}}^{\text{up}}(n_A)]$.

The number of neutrons $N_0(n_A)$ whose energy is in the range from 0 to $E_{\text{UCN}}^{\text{foil}}$ is connected to the counting rate of detector by the following relation:

$$N_0(n_A) = \frac{N_0^*(n_A)}{d_{\text{below}}(n_A)}, \quad (30)$$

where

$$d_{\text{below}}(n_A) = D_{\text{below}} \tau_{\text{stor}}^{\text{below}}(n_A) / [\tau_{\text{stor}}^{\text{below}}(n_A) + \tau_{\text{emp}}^{\text{below}}(n_A)].$$

The values $\tau_{\text{stor}}^{\text{below}}(n_A)$ and $\tau_{\text{emp}}^{\text{below}}(n_A)$ are measured at the absorber position $h = E_{\text{UCN}}^{\text{foil}}/mg$ and with removed exit foil (6 in Fig. 1). The values $\tau_{\text{stor}}^{\text{up}}(n_A)$ and $\tau_{\text{emp}}^{\text{up}}(n_A)$ are measured at the top position of the absorber when $h = E_{\text{UCN}}^{\text{trap}}/mg$ and with the entrance foil (1 in Fig. 1) at the neutron guide entrance.

The factor of the foil transmission T_{foil} is measured in the same case, comparing the measurements with and without the exit foil (6 in Fig. 1). As already mentioned, D_{up} and D_{below} for measurements with He and with ^{86}Kr are cancelled in relation (25). Thus, it is obviously possible to reach an accuracy of about 1% in the determination of the left part of Eq. (25).

VI. CONCLUSION

According to Fig. 6 we can conclude that the method of above-barrier neutrons is more sensitive with respect to the $P\tau$ method within the range of large λ values. It is concerned with the possibility of direct detection of neutrons scattered due to long-range forces. At the same time the analysis with $b = b_{\text{free-int}}$ allows us to extend considerably the range of studied λ values.

Detailed measurements of the dependence of $P_A \tau_{\text{stor}}^{\text{gas}}$ on gas pressure are necessary in order to study some possible effects of the collective interaction of UCNs with gas atoms.

To summarize it is worth noticing that the sensitivity of the proposed methods is comparable to that of methods discussed in the Introduction [9], but in this case neutrons with extremely low energy are used. The effect of long-range interaction (if it exists) can be isolated directly by means of the registration of lower-energy up-scattered neutrons. In the proposed methods we consider the interaction of neutrons with free atoms. It is important to study the long-range forces with a range exceeding the distance between atoms in materials.

ACKNOWLEDGMENTS

This work was supported by the Russian Foundation for Basic Research (Projects No. 08-02-01052a, No. 10-02-00217a, and No. 10-02-00224a), by the Federal Agency of Education of the Russian Federation (Contracts No. P2427, No. P2500, and No. P2540), and by the Ministry of Education and Science of the Russian Federation (Contracts No. 02.740.11.0532 and No. 14.740.11.0083).

-
- [1] E. G. Floratos and G. K. Leontaris, *Phys. Lett. B* **465**, 95 (1999).
- [2] A. Kehagias and K. Sfetsos, *Phys. Lett. B* **472**, 39 (2000).
- [3] I. Antoniadis, S. Dimopoulos, and G. Dvali, *Nucl. Phys. B* **516**, 70 (1998).
- [4] S. S. Gubser and J. Khoury, *Phys. Rev. D* **70**, 104001 (2004).
- [5] A. Upadhye, S. S. Gubser, and J. Khoury, *Phys. Rev. D* **74**, 104024 (2006).
- [6] E. G. Adelberger, B. R. Heckel, and A. E. Nelson, *Annu. Rev. Nucl. Part. Sci.* **53**, 77 (2003).
- [7] E. G. Adelberger, J. H. Gundlach, B. R. Heckel, S. Hoedl, and S. Schlamminger, *Prog. Part. Nucl. Phys.* **62**, 102 (2009).
- [8] Yu. Kamyshkov, J. Tithof, and M. Vysotsky, *Phys. Rev. D* **78**, 114029 (2008).
- [9] V. V. Nesvizhevsky, G. Pignol, and K. V. Protasov, *Phys. Rev. D* **77**, 034020 (2008).
- [10] Yu. N. Pokotilovski, *Yad. Fiz.* **69**, 953 (2006) [*Phys. Atom. Nucl.* **69**, 924 (2006)].
- [11] D. J. Kapner, T. S. Cook, E. G. Adelberger, J. H. Gundlach, B. R. Heckel, C. D. Hoyle, and H. E. Swanson, *Phys. Rev. Lett.* **98**, 021101 (2007).
- [12] A. A. Geraci, S. J. Smullin, D. M. Weld, J. Chiaverini, and A. Kapitulnik, *Phys. Rev. D* **78**, 022002 (2008).
- [13] J. C. Long, H. W. Chan, A. B. Churnside, E. A. Gulbis, M. C. M. Varney, and J. C. Price, *Nature (London)* **421**, 922 (2003).
- [14] B. W. Harris, F. Chen, and U. Mohideen, *Phys. Rev. A* **62**, 052109 (2000).
- [15] E. Fischbach, D. E. Krause, V. M. Mostepanenko, and M. Novello, *Phys. Rev. D* **64**, 075010 (2001).
- [16] R. S. Decca, D. Lopez, H. B. Chan, E. Fischbach, D. E. Krause, and C. R. Jamell, *Phys. Rev. Lett.* **94**, 240401 (2005).
- [17] S. K. Lamoreaux, *Phys. Rev. Lett.* **78**, 5 (1997).
- [18] M. Bordag, B. Geyer, G. L. Klimchitskaya, and V. M. Mostepanenko, *Phys. Rev. D* **58**, 075003 (1998).
- [19] J. Chiaverini, S. J. Smullin, A. A. Geraci, D. M. Weld, and A. Kapitulnik, *Phys. Rev. Lett.* **90**, 151101 (2003).
- [20] C. D. Hoyle, U. Schmidt, B. R. Heckel, E. G. Adelberger, J. H. Gundlach, D. J. Kapner, and H. E. Swanson, *Phys. Rev. Lett.* **86**, 1418 (2001).
- [21] G. L. Greene and V. Gudkov, *Phys. Rev. C* **75**, 015501 (2007).
- [22] V. F. Sears, *Phys. Rep.* **141**, 281 (1986).
- [23] V. V. Nesvizhevsky and K. V. Protasov, *Classical Quantum Gravity* **21**, 4557 (2004).
- [24] A. Serebrov, A. Vassiljev, M. Lasakov, I. Krasnoschekova, A. Fomin, P. Geltenbort, and E. Siber, *Phys. Lett. A* **367**, 268 (2007).
- [25] Yu. Yu. Kosvintsev, Yu. A. Kushnir, V. I. Morozov, and G. I. Terekhov, in *Proceedings of the 5-th All-Union Conference on Neutron Physics, Kiev, 1980*, edited by L. Usachev (TSNIAtominform, Moscow, 1980), p. 130.
- [26] D. C. Rorer, B. M. Ecker, and R. Ö. Akyüz, *Nucl. Phys. A* **133**, 410 (1969).
- [27] J. R. Stehn, M. D. Goldberg, B. A. Magurno, and R. Wiener-Chasman, *Neutron Cross Sections Z = 1 to 20*, BNL-325, 2nd ed. Suppl. 2 (U.S. Government Printing Office, Washington, 1964).
- [28] S. F. Mughabghab, M. Divadeenam, and N. E. Holden, *Neutron Cross Sections Series* (Academic, New York, 1981), Vol. 1, Part A.
- [29] H. Kaizer, H. Rauch, G. Badurek, W. Bauspiess, and U. Bonse, *Z. Phys. A* **291**, 231 (1979).
- [30] L. Koester, H. Rauch, and E. Seymann, *At. Data Nucl. Data Tables* **49**, 65 (1991).
- [31] [<http://www.ncnr.nist.gov/resources/n-lengths/>]; [http://www.atl.ac.at/~neutropt/scattering/Scattering_lengths_table_20010419.pdf].